

Phase diagram for investigating the scattering properties of passive scatterers

Jeng Yi Lee and Ray-Kuang Lee

A universal map, based on power conservation, reveals all allowable scattering states in a single plot and can be used to inversely design field-controllable structures.

The study of scattering (i.e., how a single receiver or scatterer responds to an external stimulus) is relevant to a wide range of subjects that are, in some way, related to wave physics (e.g., electromagnetic radiation, elastic waves, thermal diffusion, and quantum physics). Inspired by the recent developments of metamaterials and state-of-the-art nano-optical technologies, the design of functional scatterers has attracted much attention over the last decade (both experimentally and theoretically). For instance, unusual scattering states (including invisible cloaking, resonant scattering, coherent perfect absorption, superscattering, and superabsorbers) have been demonstrated when specific materials are used in the configuration of multilayered structures.¹⁻⁵ Devices in which these scattering states are used have great potential for applications in biochemistry, green-energy generation, ultrasensitive detection sensors, and optical microscopy. To obtain the exotic electromagnetic properties at a subwavelength scale, however, a variety of specific conditions need to be satisfied and a better understanding of scattering coefficients is thus required.

The study of light radiation being scattered from small particles can be traced back to Lord Rayleigh's explanation for the color of the sky.⁶ Furthermore, an exact solution for spherical scatterers was derived by Mie and Lorenz more than a century ago.⁷ This solution is valid for particles with any geometrical size, and for possible permittivity and permeability values. Nonetheless, although a basic understanding of the recently discovered unusual scattering states can be derived from existing scattering theory, a unified understanding of all these exotic states is still lacking.

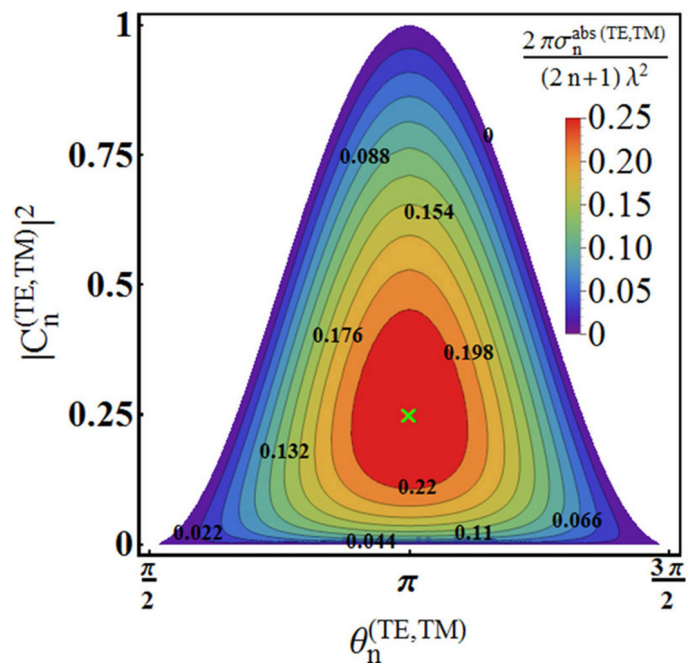


Figure 1. Phase diagram for a passive scatterer defined by the magnitude, $|C_n^{(TE, TM)}|$, and the phase, $\theta_n^{(TE, TM)}$, of the transverse electric (TE) and transverse magnetic (TM) modes of electromagnetic radiation (where n denotes the order of the harmonic channel). The colored region represents the allowable solutions of $C_n^{(TE, TM)}$ and the white region represents the forbidden states for passive scatterers. The value (i.e., color) of the contours represents the normalized absorption cross section (σ_n^{abs}) for the TE or TM modes. λ : Wavelength of electromagnetic radiation.⁸

In our work,⁸ we have therefore investigated the bounds and limits on the general scattering process for arbitrary geometries and materials. We use the amplitude and phase of scattering coefficients to produce a universal map of the electromagnetic

Continued on next page

properties of passive scatterers. We have also used this phase diagram to demonstrate a systematic method for inversely designing field-controllable structures that are based on permitted trajectories in the phase diagram (i.e., by highlighting and manipulating light scattering, absorption, and extinction). Our proposed phase diagram thus provides a simple tool for designing passive scatterers and has the potential for use in a variety of other applications, e.g., in metamaterials, acoustic physics, device fabrication, and quantum scattering systems.

We base our standard approach for dealing with scattering in the electromagnetic systems of a single scatterer (with arbitrary size and geometry) on the multipole fields expansion.⁸ The key idea in this approach is to use the orthogonal spherical harmonic functions to decompose the incident and scattered fields into multipole fields. We then use asymptotic analysis and a calculation of energy flux over a closed surface to define the relevant cross sections—i.e., absorption (σ^{abs}), scattering, and extinction—that are related to the electric and magnetic scattering coefficients, $C_{(n,m)}^{TM}$ and $C_{(n,m)}^{TE}$, respectively (where TE and TM stand for transverse electric and transverse magnetic modes, and where n and m are harmonic channel orders). We can then use the magnitude, $|C_n^{(TE,TM)}|$, and the phase, $\theta_n^{(TE,TM)}$, of the different modes to redefine the TE and TM scattering coefficients as complex scattering coefficients. When we consider the realistic material dispersion, intrinsic loss of material leads (because of causality) to an imaginary component of the material

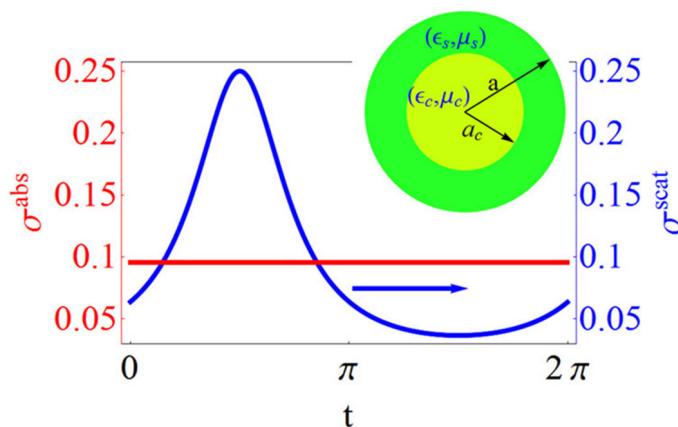


Figure 2. Absorption and scattering cross sections (σ^{abs} and σ^{scat} , respectively) for a core-shell structure (inset), as obtained from a constant absorption contour in Figure 1, shown as a function of an independent (parametric) variable. The core-shell structure is used as an example to design a passive electromagnetic device with constant absorption power. The radius of the whole structure (s) and of the core (c) is given by a and a_c , respectively. ϵ : Permittivity. μ : Permeability.⁸

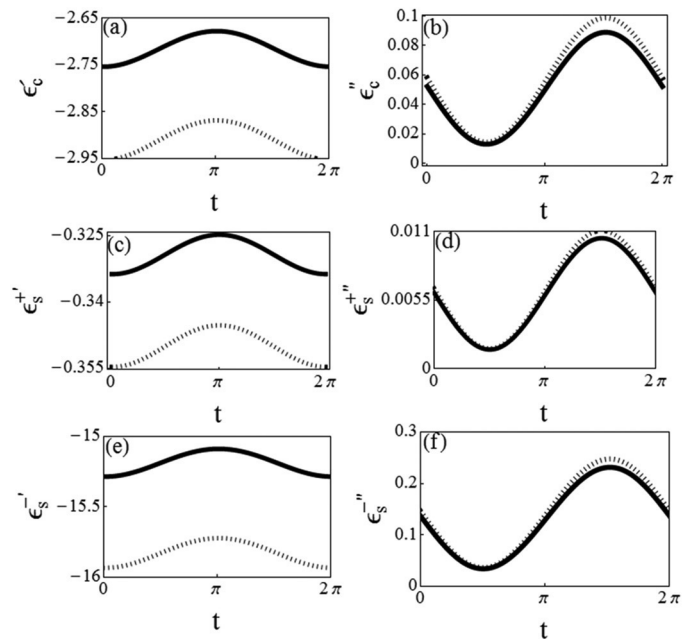


Figure 3. Calculated permittivity (ϵ) values required to support a constant absorbed power for a core-shell structure (as shown in Figure 2), where a is $\lambda/24$ and a_c/a is 0.9. In (a) and (b), ϵ_s is 3.12, and in (c) to (f) ϵ_c is 5. Analytical results (based on quasi-static limits) and exact numerical solutions (based on Mie scattering theory) are both shown, i.e., as solid and dashed lines, respectively.⁸

permittivity of the scatterer (ϵ) that is greater or equal to 0. This in turn results in $\sigma^{abs} \geq 0$ and means that power is dissipated by the scattering object. On the basis of this power conservation, we can depict the permitted and forbidden solutions for passive scatterers in the phase diagram. Our phase diagram (see Figure 1) is defined by the square of the amplitude and phase of the scattering coefficients for the electric and magnetic scattering coefficients in each spherical harmonic channel.⁸ We emphasize that no specific structures or material properties are considered in forming the phase diagram (i.e., it is based only the power conservation).

As illustrated for our phase diagram example in Figure 1, the colorful region represents the allowable solutions of $C_n^{(TE,TM)}$ and the white region represents the forbidden states for passive scatterers. All interesting and unusual scattering phenomena can be clearly represented on this single phase diagram. For example, the scattering coefficients of lossless materials embedded in arbitrary scattering objects would fall along the purple line between the loss and gain boundaries. In addition, the point

at $|C_n^{(TE, TM)}| = 1$, $\theta_n^{(TE, TM)} = \pi$ represents the maximum scattering power in each channel, which corresponds to localized surface plasmons (desirable in subwavelength nanophotonics for sensing and molecular signal enhancement) but which relies on a negative ϵ value.² The green cross at $|C_n^{(TE, TM)}| = \frac{1}{2}$, $\theta_n^{(TE, TM)} = \pi$ marks the maximum absorption power (which occurs as the outgoing wave is cancelled).³ Furthermore, minimum and maximum scattering radiations—when $\theta_n^{(TE, TM)} = \pi$ —can occur (corresponding to the conjugate matched condition) along the contour of a constant absorption power.³ With the minimum in the scattering magnitude, it is possible to design weakly disturbed scatterers without sacrificing any absorbed energy. From these examples it is thus obvious that our phase diagram for scatterers provides alternative, yet clear, information regarding the related power management.

When the geometric size of scatterers is comparable with the incident wavelength, we can approximate the scattered field by the electrical dipole model. With this model (which is applied widely in nanophotonics), the corresponding scattering power is inversely proportional to the wavelength of the fourth power, as long as there is off-resonance. By taking a core-shell structure as our example (see Figure 2), we were able to analytically reveal all the possible solutions for a constant absorbed power, but for different scattering cross sections. Moreover, with the use of geometric parameters (e.g., the size of the core-shell scatterer and the ratio of the thickness of the core radius and the whole particle), we can determine the possible permittivities required to support a constant absorption power. For example, we show analytical results (based on quasi-static limits) and exact numerical solutions (based on Mie scattering theory) as solid and dashed curves, respectively, in Figure 3. In general, it is non-trivial to determine the corresponding materials for given scattering and absorption properties. With our phase diagram for passive scatterers, however, we provide a systematic and efficient method for designing scattered-field-controllable devices. In addition, as multichannels become dominant, it is possible to display them in our phase diagram to observe their interferences and the related power distributions of the scattering patterns.

In summary, we have developed a novel phase diagram (in which intrinsic power conservation is embedded) that can be used to obtain a clear understanding of the limitations of scattering properties and the related power management. Our phase diagram does not depend on the structures of any passive isotropic scatterers. We have also demonstrated the framework for inverse design (with great potential for the realization of scattered-field-controllable devices) that is enabled with our phase diagram. Our results provide a refreshing viewpoint of the scattering phenomenon and they can be readily applied to

other wave systems. In future studies we plan to move beyond passive scatterers, and to thus consider how to manage power distribution (i.e., between dissipative and radiative losses) in the phase diagram. We will also examine the robustness of exotic scattering and absorption phenomena.

This work is supported by the Taiwan Ministry of Science and Technology.

Author Information

Jeng Yi Lee and Ray-Kuang Lee
 Institute of Photonics Technologies
 National Tsing Hua University
 Hsinchu, Taiwan

Jeng Yi Lee received his PhD from National Tsing Hua University in 2014, and is currently a postdoctoral researcher. His research interests include scattering theory, design of invisible cloaking, metamaterials, and the theory of continuum mechanics.

Ray-Kuang Lee is a professor whose research interests focus on the development of quantum-classical correspondences between optical and matter waves. He also conducts experimental and theoretical investigations to study new types of wave dynamics.

References

1. A. Alù and N. Engheta, *Achieving transparency with plasmonic and metamaterial coatings*, *Phys. Rev. E* **72**, p. 016623, 2005.
2. M. I. Tribelsky and B. S. Luk'yanchuk, *Anomalous light scattering by small particles*, *Phys. Rev. Lett.* **97**, p. 263902, 2006.
3. H. Noh, Y. Chong, A. D. Stone, and H. Cao, *Perfect coupling of light to surface plasmons by coherent absorption*, *Phys. Rev. Lett.* **108**, p. 186805, 2012.
4. Z. Ruan and S. Fan, *Superscattering of light from subwavelength nanostructures*, *Phys. Rev. Lett.* **105**, p. 013901, 2010.
5. N. M. Estakhri and A. Alù, *Minimum-scattering superabsorbers*, *Phys. Rev. B* **89**, p. 121416, 2014.
6. J. W. Strutt, *On the scattering of light by small particles*, *Philos. Mag.* **41**, pp. 447–454, 1871.
7. C. F. Bohren and D. R. Huffman, *Absorption and Scattering of Light by Small Particles*, Wiley, 1983.
8. J. Y. Lee and R.-K. Lee, *Phase diagram for passive electromagnetic scatterers*, *Opt. Express* **24**, pp. 6480–6489, 2016.